UNIVERSITI PUTRA MALAYSIA

ELECTRICAL AND MICROSTRUCTURAL PROPERTIES OF ND_2O_3, GD_2O_3 DOPED ZNO-V_2O_5-MNO_2-NB_2O_5 BASED VARISTOR CERAMICS

NOR HASANAH BINTI ISA

FS 2018 97

ELECTRICAL AND MICROSTRUCTURAL PROPERTIES OF Nd_2O_3, Gd_2O_3 DOPED ZnO-V_2O_5-MnO_2-Nb_2O_5 BASED VARISTOR CERAMICS

By

NOR HASANAH BINTI ISA

Thesis Submitted to the School of Graduate Studies, Universiti Putra Malaysia, in Fulfilment of the Requirements for the Degree of Master of Science

June 2018

Abstract of thesis presented to the Senate of Universiti Putra Malaysia in fulfilment of the requirements for the degree of Master of Science

ELECTRICAL AND MICROSTRUCTURAL PROPERTIES OF Nd_2O_3, Gd_2O_3 DOPED ZnO-V_2O_5-MnO_2-Nb_2O_5 BASED VARISTOR CERAMICS

By

NOR HASANAH BINTI ISA

June 2018

Chair: Raba'ah Syahidah Azis, PhD
Faculty: Science

The need for fabricating a reliable protection againts high voltage transients material have gained considerable attention in varistor ceramics field. Therefore, in this research, ZnO: Nd^{3+}, Gd^{3+} at different doping concentration were prepared using solid state method. This research are focuses on the fabrication and electrical characterization of rare earth oxides (REOs) of neodymium (III) oxide (Nd_2O_3) and gadolinium (III) oxide (Gd_2O_3) based ZnO ceramics. The aim of this studies are: (i) to study the effects of concentration of Nd, Gd doped in ZnO ceramics on the electrical and microstructural properties, (ii) to investigate the effect of sintering time on the electrical and microstructural properties of Nd, Gd doped in ZnO ceramics, and (iii) to study the effect of temperature degradation on the electrical properties of ceramics. The ceramics were designed according to $(97.40-x)ZnO(0.5)V_2O_5(2)\ MnO_2\ (0.1)Nb_2O_5\ (x)$REOs where x = 0.01 to 0.05 mol%. The mixed powder was ball milled, pre-sintered at 800 °C and pressed by a 3 tonne pressure to form a 15 mm diameter disc with 1 mm thick. The disc were sintered at 900 °C for 120 minutes and characterized using X-ray diffraction (XRD), scanning electron microscopy (SEM) with energy dispersive X-ray (EDX), densitometer, and current density (J) – electrical field (E) tool. The optimum doped ceramics were subjected to various sintering time from 120 to 210 minutes. The electrical degradation test were conducted on the ceramics that possessed optimum nonlinear α value with state of 0.85 E_{1mA} for 12 hours at various temperature from 80 to 110 °C. Cui *et al*. (2014) and Nahm (2013) reported that the REOs is a donor dopant promote the formation of cation vacancy and create defect which form the barrier. On the first objective, the fabrication of Nd, Gd doped ZnO based varistor ceramics increasing concentration to 0.03 mol% improve the microstructure properties that decreases the lattice parameter c to 5.2060 (Gd), 5.1982 (Nd) Å, increases density to 5.02 (Nd), 5.22 (Gd) g/cm^3, and increases the average grain size (D) to 3.54 µm (Nd) and decreases D to 3.56 µm (Gd), improve the electrical properties that increases the barrier height Φ_B to 0.886 (Nd), 0.849 (Gd) eV, as a consequence increases the nonlinear α value to 9.91 (Nd), 9.94 (Gd), with increases the breakdown voltage (E_{1mA}) value to 88.90 (Nd), 76.07 (Gd) V/mm, but decreases the leakage current density (J_L) to 0.45 (Nd), 0.33 (Gd) mA/cm^2, which is a potential material for medium voltage application. The further doping to 0.05 mol% deteriorate the electrical properties which decreases Φ_B to 0.720 (Nd), 0.641 (Gd) eV, as a consequence decreases the nonlinear α value to 7.10 (Nd), 5.86 (Gd), with decreases E_{1mA} to 70.07 (Nd), 73.40 (Gd) V/mm,

but increases J_L to 0.45 (Nd), 0.59 (Gd) mA/cm^2. The prolonged sintering time causes the decreases of nonlinear α and E_{1mA} with increasing J_L (Nahm and Shin, 2003). On the second objective, the prolonged sintering time from 120 to 210 minutes increases the lattice parameter *c* to 5.2156 (Nd), 5.2128 (Gd) Å but decreases the density to 4.74 (Nd), 4.62 (Gd) g/cm^3 and decreases *D* to 2.67 (Nd), 3.19 (Gd) μm except at 180 minutes (Gd) for lattice parameter *c*, 210 minutes for density (Nd,Gd) and *D* (Nd). The Φ_B is decreases to 0.633 (Nd), 0.563 (Gd) eV as a consequence the nonlinear α value is decreases to 5.74 (Nd), 5.10 (Gd) with decreases of E_{1mA} to 64.03 (Nd), 52.10 (Gd) V/mm with increases of J_L to 0.54 (Nd), 0.53 (Gd) mA/cm^2 with increasing time except at 180 minutes (Nd) for Φ_B and nonlinear α value, 210 minutes (Nd) for J_L value and 210 minutes (Gd) for all electrical parameter. Degradation causes the drastic increment in the J_L and reduction of nonlinear α and E_{1mA} (Abdullah *et al*., 2016). On the third objective, the degraded ZnO based varistor ceramics doped with Nd_2O_3 possessed the Negative Creep Leakage Current and increases the nonlinear α value to 6.30 with decreases J_L to 0.41 mA/cm^2 with increasing temperature from 95 to 110 °C, is better than that doped with Gd which possessed the Positive Creep Leakage Current and decreases the nonlinear α value to 3.71 with increases J_L to 0.64 mA/cm^2 at 110 °C. The minimum and maximum value of nonlinear *α* value are 5.10 and 9.94, E_{1mA} are 52.10 and 88.90 V/mm, J_L are 0.33 and 0.54 mA/cm^2, and *D* are 2.54 and 3.85 μm show the potential of this material limit. An investigation of the *J-E* characteristics for doped samples exhibited a nonohmicity depending on the REOs inclusions in the ZnO base matrix. The different proportions of the dopant constituents gave rise to different nonlinear *α*, E_{1mA}, dan J_L. The significance of Nd and Gd doping sintered at 120 minutes raised the E_{1mA} and the nonlinear *α* but lowered J_L.

Abstrak tesis yang dikemukakan kepada Senat Universiti Putra Malaysia sebagai memenuhi keperluan untuk ijazah Master Sains

SIFAT- SIFAT ELEKTRIKAL DAN MIKROSTRUKTUR DARI Gd_2O_3, Nd_2O_3 DIDOP SERAMIK VARISTOR BERASASKAN ZnO-V_2O_5-MnO_2-Nb_2O_5

Oleh

NOR HASANAH BINTI ISA

Jun 2018

Pengerusi: Raba'ah Syahidah Azis, PhD
Fakulti: Sains

Keperluan untuk fabrikasi bahan perlindung yang boleh dipercayai untuk melawan transien bervoltan tinggi telah mendapat perhatian penting dalam bidang seramik varistor. Oleh itu, dalam kajian ini, ZnO: Nd^{3+},Gd^{3+} pada kepekatan dop yang berbeza telah disediakan menggunakan kaedah keadaan pepejal. Kajian ini memfokuskan pada fabrikasi dan pencirian elektrikal terhadap oksida nadir bumi (ONB) terhadap oksida (III) neodimium (Nd_2O_3) dan oksida (III) gadolinium (Gd_2O_3) berasaskan seramik ZnO. Tujuan kajian ini ialah (i) untuk mengkaji kesan kepekatan Nd,Gd didopkan dalam seramik ZnO terhadap ciri-ciri elektrik dan mikrostruktur, (ii) untuk menyiasat kesan masa sinter terhadap ciri-ciri elektrik dan mikrostruktur Nd, Gd telah didop dalam seramik ZnO, dan (iii) untuk mengkaji kesan suhu degradasi terhadap ciri-ciri elektrik seramik. Seramik telah direkabentuk menurut (97.40-*x*)ZnO(0.5)V_2O_5 (2)MnO_2(0.1)Nb_2O_5 (*x*)ONB dimana x = 0.01 ke 0.05 mol%. Serbuk dicampur telah dikisar bebola, dipra-sinter pada 800 °C, dan ditekankan pada tekanan 3 ton untuk membentuk 15 mm diameter disk dengan ketebalan 1 mm. Disk disinter pada 900 °C selama 120 minit dan dicirikan menggunakan peralatan pembelauan sinar-X (XRD), pengimbas electron mikroskop (SEM) dengan tenaga serakan sinar-X (EDX), meter ketumpatan, dan ketumpatan arus (J) - medan elektrik (E). Seramik didopkan yang optimum telah tertakluk pada masa sinter yang pelbagai dari 120 sehingga 210 minit. Ujian degradasi elektrik telah dilakukan terhadap seramik yang mempunyai nilai α taklinear yang optimum dengan keadaan 0.85 E_{1mA} selama 12 jam pada suhu yang pelbagai dari 80 sehingga 110 °C. Cui *et al*., (2014) dan Nahm (2013) telah melaporkan bahawa ONB merupakan dopan penderma yang menggalakkan pembentukan kekosongan kation dan mewujudkan kecacatan yang membentuk halangan. Pada objektif pertama, fabrikasi Nd,Gd didopkan ZnO berasaskan varistor seramik menaikkan kepekatan kepada 0.03 mol% meningkatkan sifat mikrostruktur yang menurunkan pemalar kekisi c kepada 5.2060 (Gd), 5.1982 (Nd) Å, menaikkan ketumpatan kepada 5.02 (Nd), 5.22 (Gd) g/cm^3, menaikkan saiz bijian purata (D) kepada 3.54 μm (Nd) dan menurunkan D kepada 3.56 μm (Gd), meningkatkan ciri-ciri elektrikal yang menaikkan ketinggian halangan Φ_B kepada 0.886 (Nd), 0.849 (Gd) eV, sebagai akibatnya menaikkan nilai tidak linear α kepada 9.91 (Nd), 9.94 (Gd), dengan kenaikan nilai voltan pecah tebat (E_{1mA}) kepada 88.90 (Nd), 76.07 (Gd) V/mm, tetapi menurunkan ketumpatan arus bocor (J_L) kepada 0.45 (Nd), 0.59 (Gd) mA/cm^2, yang merupakan bahan berpotensi untuk aplikasi voltan sederhana. Doping lanjut sehingga 0.05 mol% merosakkan sifat elektrikal yang menurunkan Φ_B kepada 0.720 (Nd), 0.641

eV (Gd), sebagai akibatnya menurunkan nilai tidak linear α kepada 7.10 (Nd), 5.86 (Gd), dengan penurunan E_{1mA} kepada 70.07 (Nd), 73.40 (Gd) V/mm, tetapi menaikkan J_L kepada 0.45 (Nd), 0.59 (Gd) mA/cm^2. Masa pensinteran berpanjangan menyebabkan penurunan tidak linear α dan E_{1mA} dengan kenaikan J_L (Nahm dan Shin, 2003). Pada objektif kedua, masa pensinteran berpanjangan daripada minit 120 sehingga 210 menaikkan pemalar kekisi *c* sehingga 5.2156 (Nd), 5.2128 (Gd) Å tetapi menurunkan ketumpatan kepada 4.74 (Nd), 4.62 (Gd) g/cm^3 dan menurunkan *D* kepada 2.67 (Nd), 3.19 (Gd) µm kecuali pada 180 minit (Gd) untuk pemalar kekisi *c*, 210 minit untuk ketumpatan (Nd,Gd) dan *D* (Nd). Φ_B menurun kepada 0.633 (Nd), 0.563 (Gd) eV sebagai akibatnya nilai tidak linear α menurun kepada 5.74 (Nd), 5.10 (Gd) dengan penurunan E_{1mA} kepada 64.03 (Nd), 52.10 (Gd) V/mm dengan kenaikan J_L kepada 0.54 (Nd), 0.53 (Gd) mA/cm^2 kecuali pada 180 minit (Nd) untuk Φ_B dan tidak linear α, 210 minit (Nd) untuk nilai J_L dan 210 minit (Gd) untuk semua parameter elektrikal. Degradasi menyebabkan kenaikan mendadak dalam J_L dan pengurangan tidak linear α dan E_{1mA} (Abdullah *et al.*, 2016). Pada objektif ketiga, terdegradasi ZnO berasaskan varistor yang telah didopkan dengan Nd mempunyai mempunyai rayapan arus bocor negatif dan peningkatan nilai tidak linear α kepada 6.30 dengan penurunan J_L kepada 0.41 mA/cm^2 dengan suhu yang semakin meningkat daripada 95 kepada 110 °C, adalah lebih baik daripada yang didopkan dengan Gd yang mempunyai rayapan arus bocor positif dan penurunan nilai tidak linear α kepada 3.71 dengan kenaikan J_L kepada 0.64 mA/cm^2 pada 110 °C. Nilai minima dan maksima bagi nilai tidak linear α ialah 5.10 dan 9.94, E_{1mA} ialah 52.10 dan 88.90 V/mm, J_L ialah 0.33 dan 0.54 mA/cm^2, dan *D* ialah 2.54 dan 3.85 µm menunjukkan potensi had seramik ini. Penyiasatan pencirian *J-E* untuk sampel yang didopkan mempunyai tidak ohmisiti bergantung kepada inklusi ONB dalam matrik tapak ZnO. Perbezaan perkadaran dopan konstituen memberi kenaikan kepada berbeza tidak linear α, E_{1mA}, dan J_L. Signifikasi dop Nd dan Gd telah meningkatkan E_{1mA} and tidak linear α tetapi menurunkan J_L.

ACKNOWLDEGEMENTS

In the name of Allah, the most Merciful and Beneficent

Alhamdulillah, all praises to Allah Almighty for the strengths, guidance and blessing in completing this thesis. Special gratitude to my supervisor Dr. Raba'ah Syahidah Azis for her contact support and supervision in research, academic paper, seminar, and thesis. Special appreciate to my co-supervisor Dr. Nor Kamilah Sa'at for her support and cooperative in research, academic paper and thesis. Special thanks to Prof. Dr. Azmi Zakaria for his supervision in this research. He was always generous in sharing any useful tips about research fields Extends gratitude to Ms. AnidaZura Zulkiffli from Microscopy Unit of Institute of Bioscience, Universiti Putra Malaysia and Dr. Kok Kuan Ying from X-ray Diffraction Laboratory of Malaysia Nuclear Agency. Sincere thanks to my friends in the Photoacoustic Laboratory of Physics Department such as Rosno Kinsu, Dahiru Umaru, Raheleh Muhammadi and Zura for helping me in realizing the research. Extends thanks to my friends, Fazny, Ami, Hasni, and Ety for sharing valuable information including scholarship, academic writing, seminar and thesis. Last but not least, I would like to appreciate my beloved parents Isa Ramlan and Jamilah Kaspan, my sisters Nor Syuhaida, Sofia Noraina, Raghidatul Aizah and Saidatul Syazwani and my brother Mohamad Syafiq for give me strength and supportive to complete the study. Lastly, I would like to thank Malaysia of Higher Education through MyMaster scholarship for fees, School of Graduate studies through Grant Research Scholarship for allowance and Research Management Centre through Geran Putra – Inisiatif Putra Siswazah for research which enable me to complete my study.

I certify that a Thesis Examination Committee has met on 11 June 2018 to conduct the final examination of Nor Hasanah binti Isa on her thesis entitled "Electrical and Microstructural Properties of Nd_2O_3, Gd_2O_3 Doped ZnO-V_2O_5-MnO_2- Nb_2O_5 Based Varistor Ceramics" in accordance with the Universities and University Colleges Act 1971 and the Constitution of the Universiti Putra Malaysia [P.U.(A) 106] 15 March 1998. The Committee recommends that the student be awarded the Master of Science.

Members of the Thesis Examination Committee were as follows:

Halimah bt Mohamed Kamari, PhD
Professor
Faculty of Science
Universiti Putra Malaysia
(Chairman)

Chen Soo Kien, PhD
Associate Professor
Faculty of Science
Universiti Putra Malaysia
(Internal Examiner)

Shahrom bin Mahmud, PhD
Associate Professor
Universiti Sains Malaysia
Malaysia
(External Examiner)

RUSLI HAJI ABDULLAH, PhD
Professor and Deputy Dean
School of Graduate Studies
Universiti Putra Malaysia

Date: 22 November 2018

This thesis was submitted to the Senate of Universiti Putra Malaysia and has been accepted as fulfilment of the requirement for the degree of Master of Science. The members of the Supervisory Committee were as follows:

Raba'ah Syahidah Azis, PhD
Senior Lecturer
Faculty of Science
Universiti Putra Malaysia
(Chairman)

Nor Kamilah Sa'at, PhD
Senior Lecturer
Faculty of Science
Universiti Putra Malaysia
(Member)

ROBIAH BINTI YUNUS, PhD
Professor and Dean
School of Graduate Studies
Universiti Putra Malaysia

Declaration by graduate student

I hereby confirm that:

- this thesis is my original work;
- quotations, illustrations and citations have been duly referenced;
- this thesis has not been submitted previously or concurrently for any other degree at any other institutions;
- intellectual property from the thesis and copyright of thesis are fully-owned by Universiti Putra Malaysia, as according to the Universiti Putra Malaysia (Research) Rules 2012;
- written permission must be obtained from supervisor and the office of Deputy Vice-Chancellor (Research and Innovation) before thesis is published (in the form of written, printed or in electronic form) including books, journals, modules, proceedings, popular writings, seminar papers, manuscripts, posters, reports, lecture notes, learning modules or any other materials as stated in the Universiti Putra Malaysia (Research) Rules 2012;
- there is no plagiarism or data falsification/fabrication in the thesis, and scholarly integrity is upheld as according to the Universiti Putra Malaysia (Graduate Studies) Rules 2003 (Revision 2012-2013) and the Universiti Putra Malaysia (Research) Rules 2012. The thesis has undergone plagiarism detection software.

Signature: ________________________ Date: __________________

Name and Matric No.: NOR HASANAH BINTI ISA (GS44192)

Declaration by Members of Supervisory Committee

This is to confirm that:

- the research conducted and the writing of this thesis was under our supervision;
- supervision responsibilities as stated in the Universiti Putra Malaysia (Graduate Studies) Rules 2003 (Revision 2012-2013) are adhered to.

Signature: ______________________________
Name of Chairman of Supervisory Committee: ______________________________

Signature: ______________________________
Name of Member of Supervisory Committee: ______________________________

Signature: ______________________________
Name of Member of Supervisory Committee: ______________________________

Signature: ______________________________
Name of Member of Supervisory Committee: ______________________________

TABLE OF CONTENTS

				Page
ABSTRACT				i
ABSTRAK				iii
ACKNOWLEDGEMENTS				v
APPROVAL				vi
DECLARATION				viii
LIST OF TABLES				xii
LIST OF FIGURES				xv
LIST OF ABBREVIATIONS				xviii
LIST OF SYMBOLS				xix
CHAPTER				
1	**INTRODUCTION**			1
	1.1	Varistor		1
	1.2	ZnO		3
	1.3	Problem Statement		4
	1.4	Objective		4
	1.5	Hypotheses		5
	1.6	Scope of studies		5
2	**LITERATURE REVIEW**			6
	2.1	Introduction		6
	2.2	Classification of dopants		6
	2.3	Development of ZnO-V_2O_5-MnO_2-Nb_2O_5 ceramics		7
		2.3.1	Vanadium	7
		2.3.2	Manganese	7
		2.3.3	Niobium	8
	2.4	Rare Earth Oxides		9
3	**THEORY**			12
	3.1	Introduction		12
	3.2	Electrical Characteristics		12
	3.3	Nonlinear behaviour origin		13
	3.4	Double Schotkky Barrier Model		13
	3.5	Atomic Defect Model		14
	3.6	Degradation Mechanisms		15
		2.3.1	Degradation Process	15
		2.3.2	Recovery Process	16
	3.7	Solid State Sintering		16
4	**METHODOLOGY**			18
	4.1	Introduction		18
	4.2	Specification of composition		18
	4.3	PVA Solution Preparation		18
	4.4	Base Pellet Preparation		18
	4.5	Sample Pellet Preparation		18

4.5.1 Weighing 18
4.5.2 Milling and Drying 19
4.5.3 Sieving and Pre-sintering 19
4.5.4 Granulating and Palletizing 19
4.5.5 Sintering 20
4.6 Characterization 20
4.6.1 Density 20
4.6.2 X-ray Diffraction 20
4.6.3 Scanning Electron Microscope 20
4.6.4 Electrical Test 21
4.6.5 DC Degradation Test 22
4.6.6 Uncertainty 23

5 RESULTS AND DISCUSSION 24
5.1 Introduction 24
5.2 Nd_2O_3 Concentration 24
5.2.1 Structural Analysis 24
5.2.2 Microstructural Analysis 27
5.2.3 Electrical Analysis 30
5.3 Gd_2O_3 Concentration 34
5.3.1 Structural Analysis 34
5.3.2 Microstructural Analysis 38
5.3.3 Electrical Analysis 41
5.4 Nd_2O_3 Sintering Time 45
5.4.1 Structural Analysis 45
5.4.2 Microstructural Analysis 47
5.4.3 Electrical Analysis 52
5.5 Gd_2O_3 Sintering time 55
5.5.1 Structural Analysis 55
5.5.2 Microstructural Analysis 58
5.5.3 Electrical Analysis 62
5.6 Nd_2O_3 Degradation 65
5.7 Gd_2O_3 Degradation 70
5.8 Summary of results 75

6 SUMMARY, CONCLUSION AND RECOMMENDATIONS FOR FUTURE RESEARCH 78
6.1 Conclusion 78
6.2 Recommendation for future 79

REFERENCES 80
APPENDICES 85
BIODATA OF STUDENT 86
LIST OF PUBLICATIONS 87

LIST OF TABLES

Table		Page
1.1	Series of Littelfuse Varistors Device based on MOV technology and its parameters such as steady state applied voltage range, breakdown voltage range at 1 mA, operating ambient temperature range, and transient current surge.	3
2.1	Ceramics systems, grain size, resistivity, leakage current density, breakdown voltage, nonlinear coefficient α, sintering condition of ceramics and references	9
2.2	Ceramics systems, nonlinear coefficient α, breakdown field, grain size, leakage current density and sintering condition of Rare earth oxide doped ZnO based varistor ceramics	11
5.1	Position 2θ, *d*-spacing, lattice parameter *b* and *c*, and FWHM of ZnO-based varistor ceramics doped with Nd_2O_3 at (011) plane	27
5.2	Density (ρ), relative density (ρ_{rel}), and average grain size (D) of ZnO-based varistor ceramics doped with Nd_2O_3	30
5.3	Resistivity (ρ), Leakage Current Density (J_L), Breakdown voltage (E_{1mA}), Barrier Height (Φ_B), and Nonlinear Coefficient (α) of ZnO based varistor ceramics doped with Nd_2O_3	34
5.4	Position 2θ, *d*-spacing, lattice parameter *b* and *c*, and Full Width Half Maximum (FWHM) of ZnO-based varistor ceramics doped with Gd_2O_3 at (011) plane	38
5.5	Density (ρ), relative density (ρ_{rel}), and average grain size (D) of ZnO-based varistor ceramics doped with Nd_2O_3	41
5.6	Resistivity (ρ), Leakage Current Density (J_L), Breakdown voltage (E_{1mA}), Barrier Height (Φ_B), and Nonlin-ear Coefficient (α) of ZnO based varistor ceramics doped with Gd_2O_3	45
5.7	Position 2θ, *d*-spacing, lattice parameter b and c, and Full Width Half Maximum (FWHM) of Nd_2O_3 doped ZnO based varistor at (011) plane	47
5.8	Density (ρ), relative density (ρ_{rel}), and average grain size (D) of Nd_2O_3 doped ZnO based varistor	51
5.9	Resistivity (ρ), Leakage Current Density (J_L), Breakdown voltage (E_{1mA}), Barrier Height (Φ_B), and Nonlinear Coefficient (α) of Nd_2O_3 doped ZnO based varistor	55

5.10	Position 2θ, *d*-spacing, lattice parameter b and c, and Full Width Half Maximum (FWHM) of Gd_2O_3 doped ZnO based varistor at (011) plane	57
5.11	Density (ρ), relative density (ρ_{rel}), and average grain size (D) of Gd_2O_3 doped ZnO based varistor	62
5.12	Resistivity (ρ), Leakage Current Density (J_L), Breakdown voltage (E_{1mA}), Barrier Height (Φ_B), and Nonlinear Coefficient (α) of Gd_2O_3 doped ZnO based varistor	65
5.13	Degradation Rate Coefficient (K_T), Resistivity (ρ), Percentage Variation of Resistivity ($\%\Delta\rho$), Leakage Current Density (J_L), Percentage Variation of Leakage Current Density ($\%\Delta J_L$), Breakdown Voltage (E_{1mA}), Percentage Variation of Breakdown Voltage ($\%\Delta E_{1mA}$), Barrier Height (Φ_B), Percentage Variation of Barrier Height ($\%\Delta\Phi_B$), Nonlinear Coefficient (α) and Percentage Variation of Nonlinear Coefficient ($\%\Delta\alpha$) of Nd_2O_3 doped ZnO based varistor.	70
5.14	Degradation Rate Coefficient (K_T), Resistivity (ρ), Percentage Variation of Resistivity ($\%\Delta\rho$), Leakage Current Density (J_L), Percentage Variation of Leakage Current Density ($\%\Delta J_L$), Breakdown Voltage (E_{1mA}), Percentage Variation of Breakdown Voltage ($\%\Delta E_{1mA}$), Barrier Height (Φ_B), Percentage Variation of Barrier Height ($\%\Delta\Phi_B$), Nonlinear Coefficient (α) and Percentage Variation of Nonlinear Coefficient ($\%\Delta\alpha$) of Gd_2O_3 doped ZnO based varistor.	74
5.15	Position 2θ of (011) plane, *d*-spacing, lattice parameter b and c, and Full Width Half Maximum (FWHM) of (011) plane, Density (ρ), relative density (ρ_{rel}), and average grain size (D) of ZnO-based varistor ceramics doped with Nd_2O_3 and Gd_2O_3	75
5.16	Position 2θ of (011) plane, *d*-spacing, lattice parameter b and c, and Full Width Half Maximum (FWHM) of (011) plane, Density (ρ), relative density (ρ_{rel}), and average grain size (D) of Nd_2O_3 and Gd_2O_3 doped ZnO-based varistor ceramics	76
5.17	Resistivity (ρ), Leakage Current Density (J_L), Breakdown voltage (E_{1mA}), Barrier Height (Φ_B), and Nonlinear Coefficient (α) of ZnO-based varistor ceramics doped with Nd_2O_3 and Gd_2O_3	76
5.18	Resistivity (ρ), Leakage Current Density (J_L), Breakdown voltage (E_{1mA}), Barrier Height (Φ_B),	77

	and Nonlinear Coefficient (α) of Nd_2O_3 and Gd_2O_3 doped ZnO-based varistor ceramics	
5.19	Degradation Rate Coefficient (K_T), Nonlinear Coefficient (α) and its Percentage Variation (%$\Delta\alpha$), Barrier Height (Φ_B) and its Percentage Variation (%$\Delta\Phi_B$), Breakdown Voltage (E_{1mA}) and its Percentage Variation (%ΔE_{1mA}), Leakage Current Density (J_L) and its Percentage Variation (%ΔJ_L), Resistivity (ρ) and its Percentage Variation (%$\Delta\rho$) of Nd_2O_3 and Gd_2O_3 doped ZnO based varistor ceramics	77

LIST OF FIGURES

Table		Page
1.1	A symbol of varistor	1
1.2	Varistor Protection circuit	1
1.3	CH Varistor Series (Littelfuse,2015)	2
1.4	LV UltraMOVTM Metal Oxide Varistor Series (Littelfuse,2015)	2
1.5	A Schematic diagram of a radial leaded MOV (Vishay,2013)	2
1.6	The structure of ZnO (Rodnyi and Khodyuk, 2011)	3
3.1	Typical Varistor *J-E* curve plotted on log-log scale (Littelfuse, 2015)	12
3.2	Example of ZnO-based Varistor block model (EPCOS,2012)	13
3.3	The schematic model of Double Schotkky barrier (Gupta and Carlson, 1985)	14
3.4	The schematic model of the atomic defect (Gupta and Carlson, 1985)	14
3.5	Defect diffusion and chemical interaction during degradation (Gupta and Carlson, 1985)	16
3.6	Defect diffusion and chemical interaction during recovery (Gupta and Carlson, 1985)	16
3.7	Schematic diagram of stages in solid-state sintering (Tanaka et *al.*, 2012)	17
4.1	The flowchart of sample pellet preparation	19
4.2	The method of linear intercept for average grain size determination	21
4.3	Schematic diagram of electrical test setup	22
4.4	Schematic diagram of DC degradation test setup	23
5.1	XRD patterns of ZnO-based varistors doped with Nd_2O_3	25
5.2	Position 2θ of (011) plane and *d*-spacing dependent on Nd_2O_3 concentration	26
5.3	lattice parameter *b* and *c* dependent on Nd_2O_3 concen-tration	26
5.4	FWHM of (011) plane dependent on Nd_2O_3 concentration	27
5.5	SEM image of ZnO-based varistor ceramics doped with Nd_2O_3	27
5.6	SEM attached with EDX of ZnO-based varistor ceramics doped with Nd_2O_3	28
5.7	Density and average grain size dependent on Nd_2O_3 concentration	30
5.8	*J-E* curve of ZnO-based varistor ceramics doped with Nd_2O_3	31

5.9	Resistivity and leakage current density dependent on Nd_2O_3 concentration	32
5.10	Average grain size and breakdown voltage dependent on Nd_2O_3 concentration	32
5.11	Nonlinear α and barrier height dependent on concentration of Nd_2O_3	34
5.12	XRD patterns of ZnO-based varistors doped with Nd_2O_3	35
5.13	Position 2θ of (011) plane and *d*-spacing dependent on Gd_2O_3 concentration	36
5.14	lattice parameter b and c dependent on Gd_2O_3 concentration	36
5.15	FWHM of (011) plane dependent on Nd_2O_3 concentration	37
5.16	SEM image of ZnO-based varistor ceramics doped with Gd_2O_3	38
5.17	SEM attached with EDX of ZnO-based varistor ceramics doped with Gd_2O_3	39
5.18	Density and average grain size dependent on Nd_2O_3 concentration	40
5.19	*J-E* curve of ZnO-based varistor ceramics doped with Gd_2O_3	41
5.20	Resistivity and leakage current density dependent on Gd_2O_3 concentration	42
5.21	Average grain size and breakdown voltage dependent on Gd_2O_3 concentration	43
5.22	Nonlinear α and barrier height dependent on Gd_2O_3 concentration	44
5.23	XRD patterns of Nd_2O_3 doped ZnO-based varistor ceramics	46
5.24	Position 2θ and d-spacing of (011) plane dependent on sintering time	46
5.25	lattice parameter *b* and *c* dependent on sintering time	47
5.26	FWHM of (011) plane dependent on sintering time	47
5.27	SEM images of Nd_2O_3 doped ZnO based varistor ceramics	48
5.28	SEM attached with EDX of Nd_2O_3 doped ZnO-based varistor	49
5.29	EDX elemental map of Nd_2O_3 doped ZnO based varistor ceramics sintered at 120 and 210 minutes	50
5.30	Density and average grain size dependent on sintering time	51
5.31	*J-E* curve of Nd_2O_3 doped ZnO based varistor ceramics	52
5.32	Resistivity and leakage current density dependent on time	53

5.33	Average grain size and breakdown voltage dependent on sintering time	54
5.34	Nonlinear α and barrier height dependent on sintering time	55
5.35	XRD patterns of Gd_2O_3 doped ZnO-based varistor ceramics	56
5.36	Position 2θ and d-spacing of (011) plane dependent on sintering time	56
5.37	lattice parameter *b* and *c* dependent on sintering time	57
5.38	FWHM of (011) plane dependent on sintering time	58
5.39	SEM images of Gd_2O_3 doped ZnO based varistor ceramics	58
5.40	SEM attached with EDX of Gd_2O_3 doped ZnO-based varistor	59
5.41	EDX elemental map of Nd_2O_3 doped ZnO based varistor ceramics sintered at 120 and 210 minutes	60
5.42	Density and average grain size dependent on sintering time	61
5.43	*J-E* curve of Gd_2O_3 doped ZnO based varistor ceramics	62
5.44	Resistivity and leakage current density dependent on time	63
5.45	Average grain size and breakdown voltage dependent on sintering time	64
5.46	Nonlinear α and barrier height dependent on sintering time	65
5.47	Current density dependent on time	66
5.48	*J-E* curve of Nd_2O_3 doped ZnO based varistor ceramics	67
5.49	Resistivity and leakage current density dependent on the temperature	68
5.50	Breakdown voltage dependent on temperature	68
5.51	Nonlinear α and barrier height dependent on temperature	69
5.52	Current density dependent on time	71
5.53	*J-E* curve of Gd_2O_3 doped ZnO based varistor ceramics	72
5.54	Resistivity and leakage current density dependent on temperature	72
5.55	Breakdown voltage dependent on temperature	73
5.56	Nonlinear α and barrier height dependent on temperature	73

LIST OF ABBREVIATIONS

Ag	silver
AC	alternate current
B	boron
Ba	Barium
Bi	Bismuth
Co	Cobalt
DC	Direct current
$DyVO_4$	dysprosium vanadate
DLTS	deep level transient spectroscopy
EDX	energy dispersive X-ray
Er_2O_3	erbium oxide
$ErVO_4$	Erbium Vanadate
Gd	Gadolinium
Gd_2O_3	gadolinium (III) oxide
$GdVO_4$	Gadolinium vanadate
IBS	Institute Bioscience
J- E	current density - electric field
LED	Light Emission Diode
Mn	Manganese
MOV	metal oxide varistor
Nb	Niobium
NCLC	negative creep of leakage current
Nd	Neodymium
Nd_2O_3	neodymium (III) oxide
PCLC	positive creep of leakage current
Pr	praseodymium
Pr_6O_{11}	praseodymium oxide
PVA	polyvinyl alcohols
rpm	rotation per minute
REOs	rare earth oxides
Sb	antimony
Sc_2O_3	scandium oxide
SiC	silicon carbide
SD	standard deviation
SEM	scanning electron microscope
SM	surface mount
Sr	strontium
Tb_4O_7	terbium oxide
V	vanadium
V DC	Volt Direct Current
XRD	X-ray diffraction
Y_2O_3	yttrium oxide
ZnO	zinc oxide

LIST OF SYMBOLS

A	cross sectional area of pellet
A	Ampere
mA	milliAmpere
kA	kiloAmpere
A	Richardson's Constant
C	constant depend on *J* and *E*
D	Average Grain Size
$D_{Zn}^{\bullet}$	donor ions
E	Electric Field
E_{1ma}	Breakdown Voltage
e'	electron
eV	electronvolt
G	average grain size at time t
$Gd_{Zn}^{\bullet}$	Gd in Zn site
J	Current Density
J_L	Leakage Current Density
J_{LO}	current density at t =0
J- E	Current Density - Electric Field
K_o	preexponential constant of the material
K_t	Degradation Rate Coefficient
k_B	Boltzmann Constant
L	length of pellet
L	Random Line Length On The Micrograph
M	Magnification Of The Micrograph
n	kinetic grain growth exponent
N	Number of the Grain Boundaries Intercepted By Lines
$Nd_{Zn}^{\bullet}$	Nd in Zn site
O_O	oxygen in its oxygen site
Q	apparent activation energy
R	resistance
R	universal gas constant
r	grains per unit length
T	absolute temperature
T	absolute temperature (K),
t	time
$t^{1/2}$	stressing time
$V_O^{\bullet}$	single positive charged oxygen vacancies
$V_O^{\bullet\bullet}$	double positive charged oxygen vacancies
V_{Zn}^{x}	neutral zinc vacancy
V_{Zn}'	single negative charge zinc vacancy
V_{Zn}''	double negative charge zinc vacancy
w_{air}	weight of sample in air
w_{water}	weight of sample in water
Zn_i^{x}	neutral zinc interstitial
$Zn_i^{\bullet}$	single positive charged zinc interstitials
$Zn_i^{\bullet\bullet}$	double positive charged zinc interstitials
α	Nonlinear Coefficient
Φ_B	Barrier Height

ρ	density
ρ	resistivity
ρ_{water}	density of water
$\rho_{average}$	average density
ρ_{rel}	relative density
ΔG	free energy of segregation
ΔH	segregation enthalpy
ΔS	segregation entropy
$\%\Delta\alpha$	Percentage Variation of Nonlinear Coefficient
$\%\Delta J_L$	Percentage Variation of Leakage Current Density
$\%\Delta E_{1mA}$	Percentage Variation of Breakdown Voltage
$\%\Delta\rho$	Percentage Variation of Resistivity
$\%\Delta\Phi_B$	Percentage Variation of Barrier Height
°C	Degree Celcius
μm	Micrometre
ω	barrier width

CHAPTER 1

INTRODUCTION

1.1 Varistor

The varistor is a variable resistor that protecting direct current (DC) voltage applications from transient overvoltage by diverting it to the ground. The transients overvoltage are resulted from a sudden energy released which either previously stored or induced by heavy inductive loads or lightning strikes (Kanai *et al.*, 1985; Barrado *et al.*, 2004, Littelfuse, 2013). Varistors is also recognized as portmanteau of various resistor that exhibit an non-ohmic electrical characteristic that is similar to that of a diode (Levinson and Philipp, 1986). Figure 1.1 and 1.2 shows symbol of varistor and its application in a circuit. Littelfuse, Kemet, and Vishay are famous brands in manufacturing medium voltage varistor. The commercial varistors in markets nowadays are based on zinc oxide (ZnO) that exhibit excellent nonlinear properties compared with varistor based on silicon carbide (SiC). The SiC-based varistors have very low in nonlinear coefficient α which is between 3 to 7 while ZnO-based varistors can be in between 20 to 50 (Hozer and Holland, 1994). There are variety of varistor based on ZnO available in market such as surface mount and radial leaded. Littelfuse Inc. manufactures a few series of MOVs surface mount such as CH Series as shown in Figure 1.3 for medium voltage DC to off-line board-level protection applications. This series has a wide applied voltage range from 18 V to 369 V DC and breakdown voltage range from 22 V to 430 V DC at 1 mA (Littelfuse, 2015). Its operating temperature range is from -55 °C to +125 °C with high surge rated up to 400 A. Besides, SM7 Series is another series of Littelfuse surface mount which is designed for alternate current (AC) power meter application. The applied voltage range of SM7 series is from 50 V to 150 V AC while its breakdown voltage range is from 73 V to 735 V DC test current at 1 mA. The operating ambient temperature range is from -40 °C to 85 °C with peak pulse current of 1200 A.

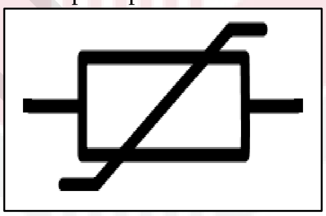

Figure 1.1: A symbol of varistor (Vishay, 2013)

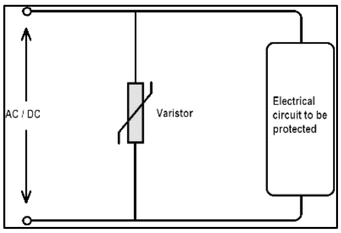

Figure 1.2: Varistor Protection circuit (Vishay, 2013)

The Littelfuse 20mm SMD Series is another surface mount MOVs device for Automotive applications with applied voltage range from 26 V to 420 V DC and breakdown voltage range from 32 V to 462 V DC at 1 mA. The operating ambient temperature range is similar to SM7 Series with peak pulse current of 6500A. In addition, the medium voltage LV UltraMOV™ Series as shown in Figure 1.4 is a Littelfuse radial leaded varistor. The series are designed for DC application such as LED lights, cordless phones, audio and video devices, mobile phone chargers, security systems, fire alarm systems, automation control systems, industrial control, contact relays, surge protection device, telecom power systems, and wireless base stations. The steady state voltage range is from 14 to 125 V DC and the breakdown voltage range is from 18 V to 68 V DC at 1 mA. The operating temperature range is from -40 °C to +125 °C and the maximum peak surge current rating can reach up to 10kA. The ZA Series of transient voltage surge suppressors are another radial leaded varistors series. It designed for use in the protection of low and medium-voltage circuits and systems such as automotive systems, motor control, solenoid, and telecom as well as power supply circuits. Its features are including wide DC voltage range from 5.5 V to 615V, breakdown voltage from 11 V to 51.7 V DC at 1 mA, and operating temperature range from -55 to +85 °C, with 50 to 6500 A. Figure 1.5 shows the schematic diagram of radial varistor where the leads and electrodes deposited on both faces of ceramics (Vishay,2013). Table 1.1 shows the series of Littelfuse varistors device and its parameters such as steady state applied voltage range, breakdown voltage range at 1 mA, operating ambient temperature range, and transient current surge.

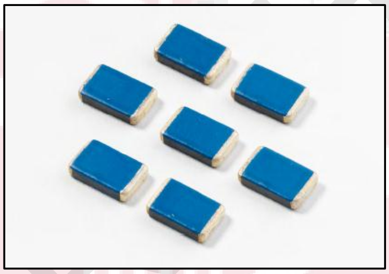

Figure 1.3: CH Varistors Series (Littelfuse, 2015)

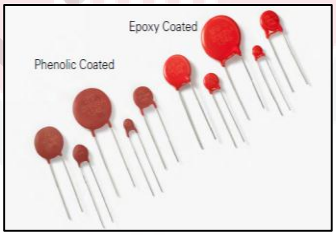

Figure 1.4: LV UltraMOV™ Metal Oxide Varistor Series (Littelfuse, 2015)

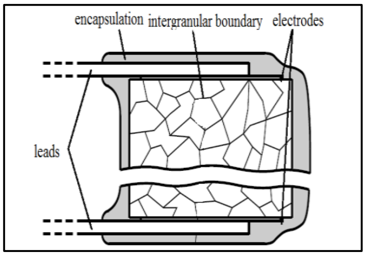

Figure 1.5: A schematic diagram of a radial leaded MOV (Vishay, 2013)

Table 1.1: Series of Littelfuse Varistors Device based on MOV technology and its parameters such as steady state applied voltage range, breakdown voltage range at 1 mA, operating ambient temperature range, and transient current surge.

Series Name	Type	Steady state applied voltage range (V DC)	Breakdown voltage range at 1 mA (V DC)	Operating Ambient Temperature Range (°C)	Transient Current surge (A)
CH	surface mount	18 to 369	22 to 430	-55 to +125	100 to 400
SM7	surface mount	50 to 150	73 to 735	-40 to +85	1200
Littelfuse 20mm SMD	surface mount	26 to 420	32 to 462	-40 to +85	6500
LV Ultra-MOV™	radial leaded	12 to 125	18 to 68	-40 to +125	500 to 10000
ZA Series	radial leaded	5.5 to 615	11 to 51.7	-55 to +85	50 to 6500

1.2 ZnO

ZnO is a wide band gap semiconductor of II-IV semiconducting group and it almost always n-type semiconductor due to presence of oxygen vacancy and zinc interstitials (Kim *et al.*, 2012). Zinc interstitial are shallow donor but high formation energy in n-type ZnO and are fast diffuser (Anderson and Chris, 2007). While the Zinc vacancy is deep acceptor and act as compensating centers in n-type ZnO. Oxygen interstitials have high formation energies and occurs as deep acceptors at octahedral interstitial sites in n-type ZnO (Anderson and Chris, 2007). Meanwhile the Oxygen vacancy is deep donors and unlikely to form because it have high formation energies in n-type ZnO. As in most II-VI materials, the hexagonal wurtzite structure is more preferred in ZnO rather than zinc blende structure (Elcombe and Kisi, 1989). This is because the structure is most common and stable at ambient conditions. ZnO is a largely ionic bond as the corresponding radii of 0.74 Å for Zn^{2+} and 1.40 Å for O^{2-}. ZnO is a polar bond since the zinc and oxygen planes are electrically charged (Elcombe and Kisi, 1989; Nirmala and Anukaliani, 2011). The insulator ZnO require high sintering temperature above 1000 °C to reveal a good electrical properties (Pandey *et al.*, 2016). The space group of ZnO is $P6_3mc$ and the lattice parameters are a is 3.25 Å and c is 5.2 Å since the structure is hexagonal. Figure 1.6 shows the hexagonal prism of the wurtzite structure of ZnO where the black and white denote Zn and O (Rodnyi and Khodyuk, 2011).

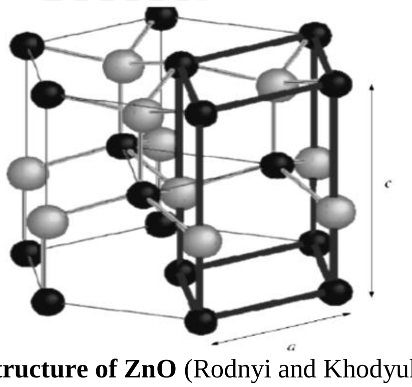

Figure 1.6: The structure of ZnO (Rodnyi and Khodyuk, 2011)

1.3 Problem statement

The semiconductor devices are very susceptible to and vulnerable to transient overvoltage. Transient overvoltage can originate from internal sources such as electrostatic discharge, switching of electrical loads, magnetic and inductive coupling, and external sources such as direct and indirect lightning (Nahm, 2013). The best way to protect DC devices is applying the ZnO based varistor into devices (Abdullah *et al.*, 2016). The rare earth oxides (REOs) doped Zn-V-Mn-Nb-O ceramics is studied recently because the ceramics exhibited the nonlinearity at low sintering temperature of 900 °C for medium voltage application (Roy *et al.*, 2018). The REOs doped Zn-V-Mn-Nb-O ceramics are very actively being studied in many aspects such as basic microstructures, nonlinear properties, dielectric characteristics, stability against DC–accelerated aging stress, and high–energy pulse current (Nahm, 2013; Roy *et al.*, 2017). The high leakage current density in medium voltage of ZnO based varistor ceramics may causes the varistor itself to easily burn. The rare earth oxides is a donor dopant in ZnO involves in the formation of cationic vacancy which defined as missing of cation from its lattice site to maintain electrical neutrality, that produce an electron deficiency and are therefore able to trap the extra electrons released by high valence dopants (Cui *et al.*, 2014, Mir-zayi and Hekmatshoar, 2013). Nahm (2013) reported that REOs with number of valence of 3 act as donor dopant in ZnO that segregate at the grain boundary create defect that form the potential barrier which inreases the nonlinear α value from 49.9 to 66.1 and the breakdown voltage from 480 to 536.5 V/mm but decreasing the leakage current density from 0.094 to 0.077 mA/cm^2 with increasing Gd_2O_3 concentration from 0 to 0.05 mol%. Therefore, the fabrication of varistor to having the low leakage current density with optimum nonlinear α value and highest breakdown voltage is necessary and worth to be investigated by using REOs with concentration below 0.05 mol%. Neodymium and Gadolinium are rare earth oxides have similar number of valence of 3 with different of ionic radii and atomic mass. The REOs doped Zn-V-Mn-Nb-O ceramics exhibited the optimum nonlinear α value at 900 °C compared to other temperatures (Nahm, 2015a; 2016). The prolonged sintering time from 0.5 to 8 hours through Zn-V-Mn-Nb-O ceramics doped with Er_2O_3 sintered at 1100 °C improve the electrical properties which increases the breakdown voltage from 197.6 to 388.0 V/mm and the nonlinear α value from 17 to 27 (Roy *et al.*, 2018). In contrast, the prolonged sintering from 1 to 3 hours for Y_2O_3 doped ZnO ceramics decreases the breakdown voltage from 194.5 to 117.4 V/mm and decreases the nonlinear α value from 51.2 to 23.8 (Nahm and Shin, 2003). Therefore, it is worth to study the effect of sintering time on the microstructures and electrical properties of varistor. Electrical degradation is another main issue in the development of varistor materials because the electrical devices operated in harsh condition at temperature range from -40 to +125 °C (Littelfuse, 2015). The prolonged or repetitive application of stresses and extreme operating condition causes the drastic increment in the leakage current density and reduction of nonlinear α and breakdown voltage (Abdullah *et al.*, 2016). Therefore, it is necessary to study the effect of electrical degradation on the electrical properties of REOs doped ZnO-based varistor ceramics.

1.4 Objective

There are three main objectives in this research work. They are;

1) to study effects of low concentrations of x mol% Nd_2O_3 and Gd_2O_3 on electrical and the microstructural properties of ZnO-based varistor ceramics fabricated

by the solid-state method at 900 °C for 120 minutes. x is 0.01,0.02,0.03,0.04, and 0.05 mol%.

2) to study effects of sintering time on the electrical and the microstructural properties of Nd_2O_3 and Gd_2O_3 doped ZnO-based varistor ceramics fabricated by the solid-state method at 900 °C for 120, 150, 180 and 210 minutes.
3) to study effects of temperature from 80 to 110 °C during direct current (DC) degradation for 12 hours on the electrical properties of the optimum of Nd_2O_3 and Gd_2O_3 doped ZnO-based varistor ceramics.

1.5 Hypotheses

There are three hypotheses in this research work.

1) The increases of Nd_2O_3 and Gd_2O_3 concentrations in the ZnO-based varistor ceramics would improve structure, microstructure and nonlinear properties of varistors. Rare earth oxide will increase the nonlinear coefficient α and breakdown voltage value but reduce the leakage current by controlling the ZnO grain growth.
2) The prolonged sintering time on Nd_2O_3 and Gd_2O_3 doped ZnO-based varistor ceramics would diminish structure, microstructure and nonlinear properties of varistors. The prolonged sintering time will reduce the nonlinear coefficient α and breakdown voltage value but increase the leakage current by controlling the ZnO grain growth.
3) The increment of ambient temperature during DC and temperature stresses would deteriorate the nonlinear properties of ZnO-based varistor ceramics. The high ambient temperature will increase the carrier generation due to Joule heating. It will causes the increase in the leakage current but the reduction in the nonlinear coefficient α and breakdown voltage value.

1.6 Scope of studies

The study is focused on the effect of Nd_2O_3 and Gd_2O_3 and sintering time on the nonlinear electrical properties such as the nonlinear coefficient α, breakdown voltage, leakage current density, resistivity, and barrier height determined from the current density-electrical field curve. For microstructure properties, the study is concerned the effect of Nd_2O_3 and Gd_2O_3 doping and sintering time on diffraction angle, *d*-spacing, lattice parameter, Full Widths Half Maximum, density, and grain size. The degradation study is limited to the leakage current creep, degradation rate coefficient K_T and percentage change of electrical parameter before and after stress based on the current density-electrical field (J-E) curve. The study is limited to the varistor ceramics prepared through conventional solid-state method and the medium voltage application.

REFERENCES

Aisah, N., Gustiono, D., Fauzia, V., Sugihartono, I., and Nuryadi, R., (2017). Synthesis and Enhanced Photocatalytic Activity of Ce-Doped Zinc Oxide Nanorods by Hydrothermal Method, IOP Conf. Ser. Mater. Sci. Eng., 172, 1-8

Abdullah, W.R.W., Zakaria, A., Hashim, M., Rahman, M.M., and Ghazali, M.S.M., (2016). Stability of ZnO-Pr_6O_{11}-Cr_2O_3 Varistor Ceramics against Electrical Degradation, Mater. Sci. Forum, 846, 115-125

Anderson, J., and Chris, V.D.W., (2007). Native point defect in ZnO, Phys. Rev. B., 76 (16), 165202, 1-22

Barrado, C.M., Leite, E.R., Bueno, P.R., Longoa, E., and Varela, J.A., (2004). Thermal conductivity features of ZnO-based varistors using the laser-pulse method, Mater. Sci. Eng. A, 371, 377-381

Chen, C.S., (2003). Effect of Dopant Valence State of Mn-Ions on the Microstructures and Nonlinear Properties of Microwave Sinteredcoble ZnO-V_2O_5 Varistors, J. Mater. Sci., 38, 1033-1038

Christen, T., Donzel, L., and Greuter, F., (2010). Nonlinear Resistive Electric Field Grading Part 1: Theory and Simulation, IEEE, 26(6), 47-59

Cui, Y., Shao, X, Prada, S., Giordano, L., Pacchioni, G., Freund, H.J., and Nilius, N., (2014). Surface Defects and their impact on the electronic structure of Mo-doped Cao films: an STM and DFT study, Phys. Chem., 16, 12764-12772

Durazzo and Riella (2008). Studies on the sintering behaviour of UO_2-Gd_2O_3 Nuclear Fuel, Proc. IYNC, 114.1-114.17

Eda, K., (1978). Conduction mechanism of non-ohmic zinc oxide ceramics, J. Appl. Phys., 49 (5), 2964-2972

Eda, K., Iga, A., and Matsuoka, M., (1980), Degradation mechanism in non-ohmic zinc oxide ceramics, J. Appl. Phys. 51, 2678-2684.

Elcombe, M.M., and Kisi, E.H. (1989). U Parameters for the Wurtzite structure of ZnS and ZnO using powder neutron diffraction. Acta Cryst. C, 45(2), 1841-2030

Emtage, P.R., (1977). The physics of zinc oxide varistors, J. Apply. Phys., 48 (10), 4372-4384

EPCOS (2012). Varistors catalog, TDK Corporation, 1-2

Ezhilvalavan, S., and Kutty, T.R.N., (1996). Dependence of non-linearity coefficients on transition metal oxide concentration in simplified compositions of ZnO + Bi_2O_3 + MO varistor ceramics (M=Co or Mn), J. Mater. Sci. Mater. Electron, 7, 137-148.

Fan, J., and Freer, R., (1994). Deep level transient spectroscopy of zinc oxide varistors doped with aluminium oxide and/or silver oxide, J. Am. Ceram. Soc., 77, 2663-2668.

Furtadoa, J.G.D.M., Saléha, L.A., Serrab, E.T., Oliveiraa, G.S.G.D., and Nóbregac, M.C.D.S., 2005. Microstructural Evaluation of Rare-Earth-Zinc Oxide-Based Varistor Ceramics, Mater. Res., 8 (4), 425-429

Ghazali, M.S.M., (2013). Characterization of zinc oxide-based varistor ceramics prepared using solid state route and co-precipitation processing. Ph.D. Thesis, Department of Physics, Universiti Putra Malaysia, Serdang, Malaysia

Ghosh, M., Karmakar, D., Basu, S., Jha, S.N., Bhattacharyya, D., Gadkari, S.C., and Gupta, S.K., (2014). Effect of size and aspect ratio on structural parameters and evidence of shape transition in zinc oxide nanostructures, J. Phys. Chem. Solids, 75(4), 543-549

Gupta, T.K., and Carlson, W.G., (1982). Barrier Voltage and its effect on Stability of ZnO Varistor. J. Appl. Phys. 53 (11), 7401-7409.

Gupta, T.K., and Carlson, W.G., (1985). A grain boundary defect model for instability/stability of a ZnO varistor. J. Mater. Sci., 20, 3487-3500

Gupta, T.K., Carlson, W.G., and Hower, P.L., (1981). Current Instability Phenomena in ZnO varistor under a continuous AC stress, J. Appl. Phys., 52(6), 4104-4111

Heiland, G., and Mollwo, E., in "Solid State Physics", edited by F. Seitz and D. Turnbull (Academic Press, New York, 1959) 8, 191-192

Hower, P.L., and Gupta, T.K., (1979). A barrier model for ZnO varistors, J. Apply. Phys., 50(7), 4847-4855

Hozer, L., and Holland, D., (1994). Semiconductor ceramics: Grain boundary effects. The University of Michigan. Ellis Horwood, 4-106

Hng, H.H., and Chan, P.L., (2004). Microstructure and current–voltage characteristics of ZnO–V_2O_5–MnO_2 varistor system, Ceram. Int., 30, 1647–1653

Hng, H.H., and Halim, L., (2003). Grain growth in sintered ZnO–1 mol% V_2O_5 ceramics. Mater. Lett., 57, 1411–1416

Hng, H.H., and Knowles, K.M., (2000). Microstructure and Current–Voltage Characteristics Multicomponent Vanadium-Doped Zinc Oxide Varistors, J. Am. Ceram. Soc., 83 (10), 2455–2462

Hng, H.H., and Tse, K.Y., (2008). Effects of MgO doping in ZnO–0.5 mol% V_2O_5 varistors, Ceram. Int., 34, 1153–1157

Kanai, H., Imai, M., and Takahashi, T., (1985). A high-resolution transmission electron microscope study of a zinc oxide varistor. J. Mater. Sci., 20, 3957-3966

Kazakey, M., Vlasova, M., Aquilar, P.A.M., Coeto, S., Tapia, R.G., and Sobolev, N.A., (2012). Reaction process in a ZnO + 1% Gd_2O_3 powder mixture during mechanical and laser processing, Mater. Sci. Eng. B, 177(16), 1417-1422

Khafagy, A.M.H., El-rabaie, S.M., Dawoud, M.T., and Attia, M.T., (2014). Microhardness, microstructure and electrical properties of ZVM ceramics, J. Adv. Ceram., 3(4), 287–296

Kim, E.D., Kim, C.H., and Oh, M.Y., (1985). Role and effect of Co_2O_3 additive on the upturn characteristics of ZnO varistors, J. Appl. Phys., 58, 3231-3235

Kim, D.H., Lee, G.W., and Kim, Y.C., (2012). Interaction of zinc interstitial with oxygen vacancy in zinc oxide: An origin of n-type doping, Solid State Commun., 152 (18), 1711-1714

Kim, B.N., Li, J.G., Suzuki, T.S., (2017). Evaluation of densification and grain-growth behaviour during sintering of zirconia, J. Ceram. Soc. Jpn., 125 (4), 357-363

Lagrange, A. (1991)., Electronic Ceramics, ed. Steele, B.C.H., Elsevier App. Sci. London and New York, 17

Lehovec, K. (1953). Space-Charge Layer and Distribution of Lattice Defects at the surfaces of Ionic Crystals. J. Chem. Phys., 21 (7), 1123-1128

Levinson, L.M., and Philipp, H.R., (1986). Zinc oxide varistor – a review, J. Am. Ceram. Soc. Bull., 65, 639–646

Lin, Y.H., Cai, J., Li, M., Nan, C.W., and He, J., (2008). Grain boundary behavior in varistor-capacitor TiO_2-rich $CaCu_3Ti_4O_{12}$ ceramics, J. Appl. Phys., 103, 1-5

Littelfuse (2013). LV UltraMOVTM Low Voltage, High Surge Current Varistor Design Guide (Preliminary Version) Littelfuse Inc. 1-27

Littelfuse (2015). Metal-oxide Varistors (MOVs) catalog, Littelfuse Inc.1-237

Liu, M., Kershhofer, L., Mosenfelder, J.L., and Rubie, D.C., (1998). The effect of strain energy on growth rate during the olivine-spinel transformation and implication

for olivine metastability in subducting slabs, J. Geophys. Res., B10(103), 23897-23909
Mantas, P.Q., and Baptista, J.L., (1995). The Barrier Height Formation in ZnO Varistors, J. Europ. Ceram. Soc., 15, 605-615
Matsuoka, M. (1971). Nonohmic Properties of Zinc Oxide Ceramics, Jpn. J. Appl. Phys., 10(6), 736-746.
Matsuoka, M., Masuyama, T., and Lida, Y., (1969). Voltage non-linearity of zinc oxide ceramics doped with alkali earth metal oxide, Jpn. J. Appl. Phys., 8, 1275-1280.
Mirzayi, M., and Hekmatshoar, M.H., (2013). Effect of V_2O_5 on electrical and micro-structural properties of ZnO ceramics, Phys. B, 414, 50–55
Masteghin, M.G., and Orlandi, M.O., (2016). Grain-boundary Resistance and Nonlinear Coefficient Correlation for SnO2-Based Varistors, Mat. Res., 19(6), 1286-1291
Mukae, K., Tsuda, K., and Nagasawa, I., (1977). Non-Ohmic Properties of ZnO- Rare Earth Metal Oxide-CO_3O_4 Ceramics, Jpn. J. Appl. Phys., 16(8), 1361-1368
Nahm, C.W. (2007). Microstructure and varistor properties of ZnO–V_2O_5–MnO_2-based ceramics, J. Mater. Sci., 42, 8370-8373
Nahm, C.W. (2009a). Effect of MnO_2 addition on microstructure and electrical properties of ZnO–V_2O_5-based varistor ceramics, Ceram. Int., 35, 541–546
Nahm, C.W. (2009b). Clamping voltage characteristics and accelerated aging behaviour of CoCrTb-doped Zn/Pr-based varistors with sintering temperature, Trans. Electr. Electr. Mater., 10 (4), 125-130
Nahm, C.W (2010). Microstructure and electrical properties of ZnO– V_2O_5– MnO_2–Co_3O_4–Dy_2O_3– Nb_2O_5-based varistors, J. Alloys Compd., 490, L52–L54
Nahm, C.W. (2011). Effect of Mn doping on electrical properties and accelerated ageing behaviours of ternary ZVM varistors, Bull. Mater. Sci., 34(7), 1385–1391.
Nahm, C.W. (2012a). Effect of sintering process on electrical properties and ageing behavior of ZnO–V_2O_5–MnO_2–Nb_2O_5 varistor ceramics, J. Mater. Sci. Mater. Electron, 23, 457-463
Nahm, C.W. (2012b). Nb_2O_5 doping effect on electrical properties of ZnO–V_2O_5–Mn_3O_4 varistor ceramics, Ceram. Int., 38, 5281-5285
Nahm, C.W. (2013). Effect of gadolinia addition on varistor characteristics of vanadium oxide–doped zinc oxide ceramics, J. Mater. Sci. Mater. Electron, 24, 4839-4846
Nahm, C.W. (2015a). Effect of small changes in sintering temperature on varistor properties and degradation behaviour of V-Mn-Nb-Gd co-doped zinc oxide ceramics. Trans. Nonferrous Met. Soc. China, 23, 58-62
Nahm, C.W. (2015b). Nonohmic properties of V/Mn/Nb/Gd co-doped zinc oxide semiconducting varistors with low-temperature sintering process, Mater. Sci. Semicond. Process., 23, 58-62
Nahm, C.W. (2016). Sintering temperature dependence on microstrucutre and nonohmic properties of ZVMND ceramic semiconductors, J. Mater. Sci. Mater. Electron, 27, 9520-9525
Nahm, C.W., and Park, C.H., (2000). Microstructure, electrical properties, and degradation behavior of praseodymium oxides-based zinc oxide varistors doped with Y_2O_3. J. Mater. Sci. Lett., 35, 3037 – 3042
Nahm, C.W. and Shin, B.C., (2003). Highly stable nonlinear properties of ZnO–Pr_6O_{11}–CoO–Cr_2O_3–Y_2O_3-based varistor ceramics. Mater. Lett., 57, 1322–1326
Nahm, C.W., and Shin, B.C., (2004). Effect of sintering time on electrical properties and stability against DC accelerated aging of Y_2O_3-doped ZnO-Pr_6O_{11}-based varistor ceramics, Ceram. Int. 30, 9–15

Nahm, C.W., Park, C.H., and Yoon, H.S., (2000). Microstructure and varistor properties of ZnO-Pr_6O_{11}-CoO-Nd_2O_3 based ceramics, J. Mater. Sci. Letters, 19, 271– 274
Nirmala, M., and Anukaliani, A., (2011). Characterization of undoped and Co-doped ZnO nanoparticles synthesized by DC thermal plasma method. Physica B, 406, 911–915
Orman, J.A.V., and Crispin, K.L., (2010). Diffusion in Oxides, Rev. Mineral. Geochem., 72, 757-825
Pandey, S., Kumar, D., and Parkash, O., (2016a). Investigation of the electrical properties of liquid-phase sintered ZnO–V_2O_5 based varistor ceramics using impedance and dielectric spectroscopy, J. Mater. Sci: Mater Electron., 27, 3748-3758
Pandey, S., Kumar, D., and Parkash, O., (2016b). Electrical impedance spectroscopy and structural characterization of liquid-phase sintered ZnO–V_2O_5–Nb_2O_5 varistor ceramics doped with MnO, Ceram. Int., 42(8), 9686–9696
Park, J.H., and Nahm, C.W., (2015). Sintering effect on electrical properties and aging behaviour of quaternary ZnO–V_2O_5–Mn_3O_4–Nb_2O_5 ceramics, J. Mater. Sci. Mater. Electron, 26, 168–175
Pillai, S.C., Kelly, J.M., Ramesh, R., and McCormack, D.E., (2013). Advances in the synthesis of ZnO nanomaterials for varistor devices. J. Mater. Chem., 1, 3268-3281
Ray, A., Behera, B., Basu, T., Vajandar, S., Sapathy, S.K., and Nayak, P., (2018). Modification of structural and dielectric properties of polycrystalline Gd-doped BFO-PZO, J. Adv. Dielect., 8(4), 1-21
Rodnyi, P.A., and Khodyuk, I.V., (2011). Optical and Luminescence Properties of Zinc Oxide. Opt. Spectros., 111 (5), 776-785
Roy, S., Das, D., and Roy, T.K., (2017). Processing, characterization and properties of Er_2O_3 added ZnO based varistor ceramics, J. Mater. Sci. Mater. Electron, 28, 14906-14918
Roy, S., Roy, T.K., and Das, D., (2018). Microstructure and Current-Voltage Characteristics of Erbium Oxide Doped Multicomponent Zinc Oxide Varistor, IOP Conf. Ser. Mater. Sci. Eng., 338, 012046
Sukkar, M.H., and Tuller, H.L., in "Grain Boundaries and Interfaces in Ceramics", Adv. Ceram., Vol. 7, edited by M. F. Yan and A.H. Heuer, (American Ceramic Society, Columbus, Ohio, 1983) 71-90.
Tanaka, H., Yamamoto, A., Shimoyama, J., Ogino, H., and Kishio, K., (2012). Strongly connected ex situ MgB_2 polycrystalline bulks fabricated by solid-state self-sintering, Supercond. Sci. Technol. 25, 115022-115028
Thomas, D.G., (1957). Interstitial Zinc in Zinc Oxide, J. Phys. Chem. Solids, 3, 229-237
Thűmmler, F., and Thomma, W., (1967). The sintering process. Metall. Rev., 115, 69-108
Tsai, J.K., and Wu, T.B., (1996). Microstructure and nonohmic properties of binary ZnO-V_2O_5 ceramics sintered at 900 °C, Mater. Lett., 26, 199-203
Uric, P.A., and Notis, M.R. (1973). Final – Stage Densification During Pressure-Sintering of CoO, J. Am. Ceram. Soc., 56(11), 570-574
Vishay (2013). Varistors Introduction, Technical Note, Vishay BCComponents, 1-12
Vijayaprasath G., Murugan, R., Hayakawa, Y., and Ravi, G., (2016). Optical and magnetic studies on Gd doped ZnO nanoparticles sysnthesized by co-precipitation method, J. Lumin., 178, 375-383
Wang, C.M., Zang, G., and Wang, C., (2005). Nonlinear Electrical Characteristics of SnO2-CuO Ceramics with Different Donors, J. App. Phy., 97, 126103, 1-3

Wang, M.H., Hu, K.A., Zhao, B.Y. and Zhang, N.F. (2007). Degradation phenomena due to humidity in low voltage ZnO varistors, Ceram. Int., 33, 151-54.

Wang, M.H., Tang, Q.H., and Yao, C., (2010). Electrical properties and AC degradation characteristics of low voltage ZnO varistors doped with Nd_2O_3, Ceram. Int., 36, 1095–1099

Wong, J., (1975). Microstructure and Phase Transformation in a Highly Non-ohmic Metal Oxide Varistor Ceramic, J. Appl. Phys., 46, 1653-1659

Wurst, J.C., and Nelson, J.A., (1972). Linear Intercept Technique for Measuring Grain Size in Two-phase Polycrystalline Ceramics. J. Am. Ceram. Soc., 55(2), 109

Yan, J.K., Kang, K.Y., Du, J.H., and Yi, J.H., (2016). Grain boundary segregation and secondary-phase transition of (La,Nb)-codoped TiO_2 ceramics, Ceram. Int., 42(10), 11584-11592

Zahid, R., Azmi, Z., and Sabri, M.G.M., (2011). Photopyroelectric Spectroscopic Studies of ZnO-MnO_2–Co_3O_4 –V_2O_5 Ceramics, Int. J. Mol. Sci., 12(3), 1625-1632

Zhoa, Y., Song, S., Si, H., and Wang, K. (2017). Effect of Grain Size on Grain Boundary Segregation Thermodynamics of Philosophyin Interstitial-Free and 2.25Cr-1Mo Steels, Metals, 470(7),1-16

Zhou, D., Zhang, C., and Gong, S., (2003). Degradation phenomena due to dc bias in low-voltage ZnO varistors, Mater. Sci. Engin., B99, 412-415

BIODATA OF STUDENT

Nor Hasanah binti Isa was born on 1st June 1992. She is currently residing at Melaka. She previsely was a student of Universiti Putra Malaysia and obtained Bachelor of Science with honours major Physics. She is at present a Master Student of Universiti Putra Malaysia in Advanced Material.

LIST OF PUBLICATIONS

Isa, N.H.*, Zakaria, A., Azis, R.S., and Abdullah, W.R.W., (2017). Microstructure and Nonlinear Properties of Zn-V-Mn-Nb-O Varistor Ceramics with Nd_2O_3 Substitution, Digest Journal of Nanomaterials and Biostructures, 12 (3), 821-827

Isa, N.H.*, Zakaria, A., Azis, R.S., and Rizwan, Z., (2017). Microstructural and Nonlinear Properties of Zn-V-Mn-Nb-O Varistor Ceramics with Gd_2O_3 Substitution for Low Voltage Application, Solid State Phenomena**,** 268, 181-185

Isa, N.H.*, Azis, R.S., and Sa'at, N.K., (2018). The effect of sintering time on the microstructural and nonlinear electrical properties of Zn-V-Mn-Nb-Nd-O low-voltage varistor ceramics, J. Phys.: Conf. Ser., 1083 (012009), 1-6

Isa, N.H.*, Azis, R.S., Sa'at, N.K., Zakaria, A., Mohammadi, R., and Kinsu, R.,(2018). The effect of sintering time on the microstructural and nonlinear electrical properties of Zn-V-Mn-Nb-Gd-O low-voltage varistor ceramics. Emerging Themes In Fundamental and Applied Sciences-Physics, Serdang, Selangor: UPM Press. Retrieved from http://www.science.upm.edu.my/ebook-3213, 74-81

Kinsu, R., Zakaria, A., Sa'at, N.K., Azis, R.S., and Isa, N.H.* (2017). Effect of optical properties of graphene oxide reduction with difference source exposed light of uv light and laser radiation. (submitted)

Isa, N.H.*, Azis, R.S., Sa'at, N.K., and Mohammadi, R. Temperature stresses effect on the optimum nonlinear properties of ZnO-V_2O_5-MnO_2-Nb_2O_5-Gd_2O_3 Low-Voltage Varistor Ceramics, Malaysian Science and Technology Congress (MSTC2017) 2017 (Submitted)

UNIVERSITI PUTRA MALAYSIA

STATUS CONFIRMATION FOR THESIS / PROJECT REPORT AND COPYRIGHT

ACADEMIC SESSION: _______________

TITLE OF THESIS / PROJECT REPORT:

ELECTRICAL AND MICROSTRUCTURAL PROPERTIES OF Nd_2O_3, Gd_2O_3 DOPED ZnO-V_2O_5-MnO_2-Nb_2O_5 BASED VARISTOR CERAMICS

NAME OF STUDENT:

NOR HASANAH BINTI ISA

I acknowledge that the copyright and other intellectual property in the thesis/project report belonged to Universiti Putra Malaysia and I agree to allow this thesis/project report to be placed at the library under the following terms:

1. This thesis/project report is the property of Universiti Putra Malaysia.

2. The library of Universiti Putra Malaysia has the right to make copies for educational purposes only.

3. The library of Universiti Putra Malaysia is allowed to make copies of this thesis for academic exchange.

I declare that this thesis is classified as:

*Please tick (√)

☐	**CONFIDENTIAL**	(Contain confidential information under Official Secret Act 1972).
☐	**RESTRICTED**	(Contains restricted information as specified by the organization/institution where research was done).
☐	**OPEN ACCESS**	I agree that my thesis/project report to be published as hard copy or online open access.

This thesis is submitted for:

☐ **PATENT** Embargo from ____________ until ____________
(date) (date)

Approved by:

____
(Signature of Student)
New IC No/ Passport No.: 920601-06-5152

Date :

____
(Signature of Chairman
of Supervisory Committee)
Name:

Date :

[Note : If the thesis is CONFIDENTIAL or RESTRICTED, please attach with the letter from the organization/institution with period and reasons for confidentially or restricted.]